edges. The occurrence frequency, however, is significantly reduced compared to that shown in Fig. 2a.

Figure 3 shows test sample 2 after testing. Note the dark spots on the Kapton substrate along the cell periphery. Carbonization spots accumulate with each arc discharge. These spots are more pronounced for the insulated interconnectors than for the exposed silver bus bars. Thus, our experiments emphasize the reduced importance of the fields around the interconnectors. The generation of new arc centers gradually leads to a continuous degradation of the Kapton. With the associated carbonization, the initial insulation property of the substrate is lost. Hence, a typical resistance measured between the interconnector and a carbonized and, thus, the conductive Kapton spot is less than 100 Ω. Hence, the long-term exposure of solar arrays under such conditions will lead to permanent short circuits and, eventually, a complete solar array power loss.

Summary

The results of our ground tests indicate a new failure mode in the negative voltage range. Our experiments showed local arcing at solar cell edges, and, hence, they differ substantially from other experiments, where arcing was observed near the interconnectors.[1,8] In our experiments, only three arcing events were identified close to the interconnectors. Since these locations also involved a part of the solar cell edge, the influence of the corresponding interconnectors on the arcing is uncertain.

The characteristics of arcing, as observed in our experiments, can be summarized as follows.

1) Arc discharges were mainly observed between the solar cell edge region and the Kapton foil starting at voltages of −200 V.

2) Within the duration of our experiments (30 s), there is a voltage and density dependent threshold for arcing.

3) Arc discharges only occur once at a given location.

4) With the onset of arcing, the whole test sample becomes more susceptible to arcing at lower voltages.

5) There is no information on arcing effects under long-term exposure conditions (longer than 30 s). However, our tests suggest the possibility of arcing for lower applied voltages with a reduced frequency.

An understanding of the interaction processes leading to arcing is far from complete. More experimental and theoretical work is needed. Experimentally, the long-term behavior at lower voltages (−150, −100 V) should be studied. High-time resolution measurements of the current transients related to arcing will allow the study of the structures of these processes in more detail.

Quantitative theoretical studies of negatively biased solar arrays in the LEO plasma environment are required. For a comprehensive picture of arcing phenomena, the electric fields in two regions on the solar array are of interest: 1) the negatively biased interconnector and the dielectric cover glasses (coated with MgF2) of the adjacent solar cells and 2) the solar cell edge region involving the solar cell with cover glass material, the antireflection coating MgF2, the semiconductive material, the biased metallic grid fingers, and the Kapton foil.

The capability of particle-in-cell simulations to elucidate array-plasma interactions has been shown for the positive voltage range.[3,4] Similar model calculations can be designed for negatively biased arrays. They require an appropriate formulation of the relevant electrical boundary conditions and the particle environment. For the actual case, it will also be necessary to systematically study the influence of secondary particle populations on the electric field distribution.

References

[1]Stevens, N. J., "Review of Biased Solar-Array-Plasma Interaction Studies," NASA TM 82693, 1981.

[2]Thiemann, H., and Bogus, K., "High-Voltage Solar Cell Modules in Simulated Low-Earth-Orbit Plasma," *Journal of Spacecraft and Rockets,* Vol. 25, No. 4, 1988, pp. 278–285.

[3]Thiemann, H., and Schunk, R. W., "Sheath Formation Around Biased Interconnectors and Current Collection in a LEO-Plasma as Seen by PIC Simulations," *Journal of Spacecraft and Rockets* (to be published).

[4]Thiemann, H., Schunk, R. W., and Gerlach, L., "Solar Arrays in the LEO-Plasma Environment: A Model for Leakage Current Phenomena Deduced from Experimental and Theoretical Studies," *Proceedings of the European Space Power Conference,* Madrid, ESA SP-294, 1989, pp. 809–814.

[5]Thiemann, H., "Theoretical and Experimental Investigation on Leakage Current Phenomena," Final Report ESA Contract No. 6469/85/NL/RE (Rider No. 3), Freiburg, FRG, May 1989.

[6]Metz, R. N., "Circuit Transients due to Arcs on a High-Voltage Solar Array," *Journal of Spacecraft and Rockets,* Vol. 23, No. 5, 1986, pp. 499–504.

[7]Hastings, D. E., Weyl, G., and Kaufman, D., "A Simple Model for the Threshold Voltage for Arcing on Negatively Biased High Voltage Solar Arrays," *Journal of Spacecraft and Rockets* (submitted for publication).

[8]Jongeward, G. A., Katz, I., Mandell, M. J., and Parks, D. E., "The Role of Unneutralized Surface Ions in Negative Potential Arcing," *Proceedings of the IEEE Nuclear and Space Radiation Effects Conference,* Inst. of Electrical and Electronics Engineers, New York, 1985, pp. 4087–4091.

Color reproduction courtesy of Utah State University

Experimental Base Pressure Histories with Nonsteady Discrete Bleed Rates

M. J. Marongiu*
University of Illinois at Urbana-Champaign, Urbana, Illinois 61801

Nomenclature

D_N = nozzle diameter
D_S = shroud diameter
L = shroud length
M = nozzle exit Mach number
P_b = base pressure
P_0 = nozzle stagnation pressure
t = time
V_b = base additional volume

Introduction

INTERNAL and external base flows have been studied and reported extensively in the literature over the last 50 years, particularly at transonic and supersonic speeds. However, the vast majority of these studies involve steady conditions, either upstream of the separation point or at the base region.

There are flow situations in which unsteady conditions prevail, for example, nonsteady plume-wall interactions during

Received Dec. 4, 1989.

*Graduate Research Assistant, Mechanical and Industrial Engineering Department, Gas Dynamics Laboratory; currently, Visiting Assistant Professor, Mechanical Engineering Department, Texas A&M University, College Station, TX 77843.

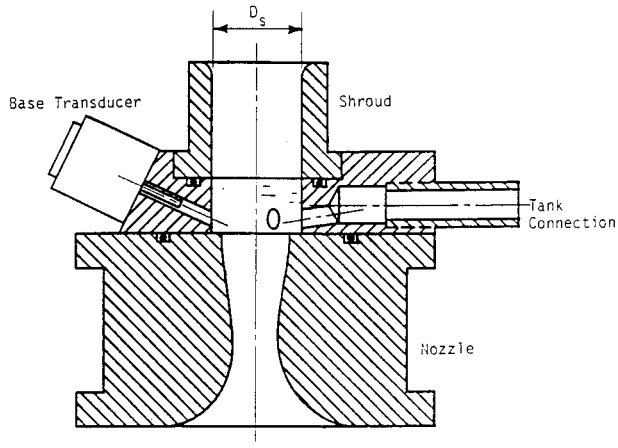

Fig. 1 Sketch of short-shroud and nozzle assembly.

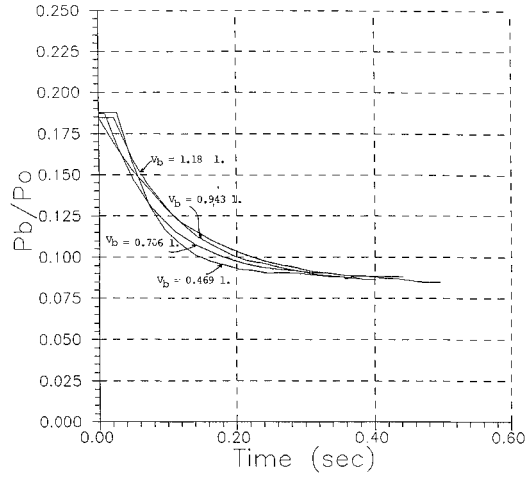

Fig. 3 Base pressure histories as a function of additional volumes with L = 1.25 in. and P_0 = 45 psig.

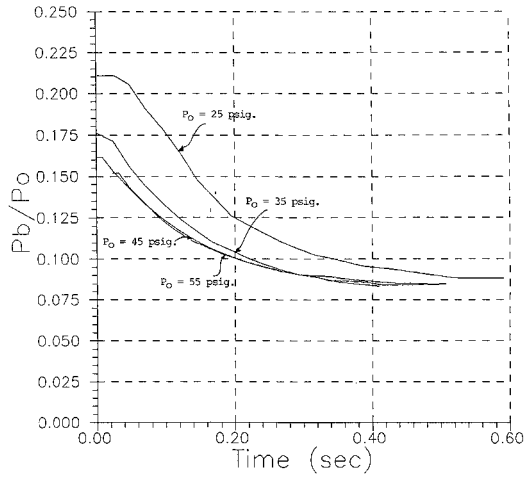

Fig. 2 Base pressure histories as a function of stagnation pressures with V_b = 1.18 liter and L = 2.25 in.

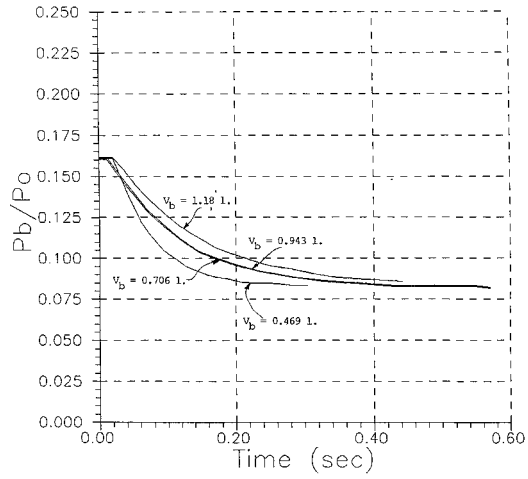

Fig. 4 Base pressure histories as a function of additional volumes with L = 2.25 in. and P_0 = 45 psig.

the early phases of the launch of small rockets in nontipoff canisters[1,2] and supersonic ejectors with unsteady secondary conditions. Here the base pressure may change as a function of the flow dissipative mechanisms. In addition, transonic and supersonic quasisteady base flow processes are controlled by the mass entrainment characteristics of the expanding shear, rather than pressure waves from the external flow,[3] which allows for adequate treatment of the problem.[1]

There is a need to obtain experimental base pressure histories with constant and varying mass injection (negative bleeds) into the base to extend the length of pulldown or to study unsteady ejector behavior. This information can be used, for example, to learn more about mass-entrainment characteristics of the shear layer and corroborate analytical treatment of the unsteady base pressure problem. This short note presents the results of an experimental investigation to obtain base pressure histories as a function of varying negative base bleed (injection) rates.

Experimentation

The experimental setup consisted of an axisymmetric converging-diverging (M = 1.55) nozzle discharging into a short shroud of larger but constant cross section. The nozzle exit diameter D_N was 0.6 in. and the shroud diameter D_S, 0.8 in. A two-dimensional setup was not chosen to lessen wall-boundary layer effects for small test sections. To investigate entrainment rates in detail, the base volume was varied by connecting a small tank of varying volume through two small rubber hoses (3/8 in. i.d.) to two 1/8 diam holes at the base. The external tank had the provision of being open to the atmosphere through a valve. The hoses reached the base area at two points not placed symmetrically. A pressure transducer was placed in the opposite side from the hose connections in the base area. The effect of shear-layer length was studied by having base evacuation with 2 shroud lengths (L = 1.25 and 2.25 in.). Figure 1 shows a sketch of the test configuration.

Evacuation was initiated by arriving at a "snap" condition.[4] While keeping the tank open to the atmosphere, the supersonic jet emerging from the nozzle expands isentropically until it satisfies the base-to-exit-nozzle-pressure ratio. This ratio is controlled by the mass inflow from the tank as the air is throttled through the valve and the shear-layer mass entrainment. The "snap" is reached by suddenly closing off the valve from the atmosphere. The base pressure decreases due to fluidic entrainment as the tank is being evacuated, and the bleed rates are controlled by the tank evacuation process. A "snap" could also occur if the upstream stagnation pressure is increased.[4]

The parameters varied in these tests were additional base volume (V_b = 1.18, 0.943, 0.706, and 0.469 liters), shroud lengths (L = 1.25 and 2.25 in.), and nozzle stagnation pressure (P_0 = 25, 35, 45, 55, 65 psig). The transient base pressures were digitally recorded. In all of the experiments, the pressure difference between the tank and the base area was 1 psia.

Results and Discussion

Representative results are now presented. Figure 2 shows base pressure histories for the short shroud (L = 1.25 in.) and largest additional volume (1.18 liter) as a function of the

nozzle stagnation pressure. The results for the effect of the additional base volume for the two shroud lengths taken at $P_0 = 45$ psig are presented in Fig. 3 for $L = 1.25$ in. and in Fig. 4 for $L = 2.25$ in.

The stagnation pressure is shown to affect the initial pressure ratio indicating the transition from overexpanded flow to underexpanded as the stagnation pressure increases. Once the flow is underexpanded, the base histories are essentially similar. The effect of shroud length, however, is more informative. The longer shroud enables the process to begin at lower pressure ratios suggesting that there is more mass entrainment since the shear layer is longer. The final base pressures are essentially identical as expected.

The role of the additional volume, based on Figs. 3 and 4, apparently is not sharply defined. Nondimensionalization of the base pressure histories using standard tank evacuation characteristic times (based on tank volume, discharge area, and speed of sound) did not make the data collapse into one trace. This suggests that the asymmetrical placement of the bleed locations and the pressure transducer may allow for nonuniform pulldown of the axisymmetric shear layer. Furthermore, the fact that there is a pressure drop across the tank connection indicates that there is a built-in impedance that affects bleed rates. In general, all experiments show that the pulldown times have been lengthened by one order of magnitude as compared with data obtained without additional base volumes.[1]

Conclusion

The experiment generated useful information regarding the effect of shroud length and thus shear-layer length. However, the results of the effect of added volume indicate that the asymmetrical placement of the tank connection does affect the base pressure histories.

Acknowledgments

This work was supported in part by the U.S. Army Research Office Grant DAAG 29-79-C-0184. The author would like to thank University of Illinois student assistants C. Grandone, J. Metcalf, and J. Slaney for their help.

References

[1]Marongiu, M. J., "Mechanisms Controlling Nonsteady Plume-Wall Interactions in Rocket Launch Tubes," Ph.D. Dissertation, Dept. of Mechanical and Industrial Engineering, Univ. of Illinois at Urbana-Champaign, Urbana, IL, July 1985.

[2]Marongiu, M. J., Korst, H. H., and White, R. A., "Nonsteady Plume-Wall Interactions in Rocket Launch Tubes," *Journal of Spacecraft and Rockets*, Vol. 25, No. 3, May-June 1988, pp. 209–216.

[3]Ihrig, H. K., Jr., and Korst, H. H., "Quasi-Steady Aspects of the Adjustment of Separated Flow Regions to Transient External Flows," *AIAA Journal*, Vol. 1, 1963, pp. 934–936.

[4]Korst, H. H., and White, R. A., "Side Vector Control Through Jet Wall Interactions in Segmented Ejector Nozzles," Mechanical and Industrial Engineering, Univ. of Illinois at Urbana-Champaign, Rept., Urbana, IL, Sept. 1973.

Errata

Tumble Orbit Transfer of Spent Satellites

Tetsuo Yasaka
Nippon Telegraph and Telephone Corporation
Yokosuka, Japan

[JSR 27, 348–350 (1990)]

DURING production of the note, five equations were inadvertently altered. On page 349, Eqs. (4) and (5) should read:

$$V_1 = V_c - 3\Delta V - \gamma_2 l\phi = V_c - (3\gamma_1 + \gamma_2)\Delta V_1 \quad (4)$$

$$V_2 = V_c - 3\Delta V + \gamma_1 l\phi = V_c - 2\gamma_1 \Delta V_1 \quad (5)$$

The following lines and Eqs. (6) and (7) on page 349 should read:

At the perigee, where the orbital velocity is $V_c + \Delta V$, the instantaneous velocities for each mass are

$$V_1 = V_c + \Delta V - \gamma_2 l\phi = V_c + (\gamma_1 - \gamma_2)\Delta V_1 \quad (6)$$

$$V_2 = V_c + \Delta V + \gamma_1 l\phi = V_c + 2\gamma_1 \Delta V_1 \quad (7)$$

On page 350, Eq. (9) should read:

$$[1 + (\gamma_2 - \gamma_1)]\Delta V_1 = 2\gamma_2 \Delta V_1 \qquad (\gamma_1 < \gamma_2) \quad (9)$$